HHS Public Access

Author manuscript

Brain Behav Immun. Author manuscript; available in PMC 2022 January 01.

Published in final edited form as:

Brain Behav Immun. 2021 January ; 91: 437–450. doi:10.1016/j.bbi.2020.11.001.

Myelin as a regulator of development of the microbiota-gut-brain axis

Ciara E. Keogh[a,1], **Danielle H.J. Kim**[a,1], **Matteo M. Pusceddu**[a,2], **Trina A. Knotts**[b], **Gonzalo Rabasa**[a], **Jessica A. Sladek**[a], **Michael T. Hsieh**[a], **Mackenzie Honeycutt**[a,b], **Ingrid Brust-Mascher**[a], **Mariana Barboza**[a], **Mélanie G. Gareau**[a,*]

[a]Department of Anatomy, Physiology and Cell Biology, School of Veterinary Medicine, University of California Davis, Davis, CA, USA

[b]Department of Molecular Biosciences, School of Veterinary Medicine, University of California Davis, Davis, CA, USA

Abstract

Myelination in the peripheral and central nervous systems is critical in regulating motor, sensory, and cognitive functions. As myelination occurs rapidly during early life, neonatal gut dysbiosis during early colonization can potentially alter proper myelination by dysregulating immune responses and neuronal differentiation. Despite common usage of antibiotics (Abx) in children, the impact of neonatal Abx-induced dysbiosis on the development of microbiota, gut, brain (MGB) axis, including myelination and behavior, is unknown. We hypothesized that neonatal Abx-induced dysbiosis dysregulates host-microbe interactions, impairing myelination in the brain, and altering the MGB axis. Neonatal C57BL/6 mice were orally gavaged daily with an Abx cocktail (neomycin, vancomycin, ampicillin) or water (vehicle) from postnatal day 7 (P7) until weaning (P23) to induce gut dysbiosis. Behavior (cognition; anxiety-like behavior), microbiota sequencing, and qPCR (ileum, colon, hippocampus and pre-frontal cortex [PFC]) were performed in adult mice (6–8 weeks). Neonatal Abx administration led to intestinal dysbiosis in adulthood, impaired intestinal physiology, coupled with perturbations of bacterial metabolites and behavioral alterations (cognitive deficits and anxiolytic behavior). Expression of myelin-related genes (*Mag, Mog, Mbp, Mobp, Plp*) and transcription factors (*Sox10, Myrf*) important for oligodendrocytes were significantly increased in the PFC region of Abx-treated mice. Increased myelination was confirmed by immunofluorescence imaging and western blot analysis, demonstrating increased expression of MBP, SOX10 and MYRF in neonatally Abx-treated mice compared to sham controls in adulthood. Finally, administration of the short chain fatty acid butyrate following completion of the Abx treatment restored intestinal physiology, behavior, and myelination impairments, suggesting a critical role for the gut microbiota in mediating these effects. Taken together, we identified a long-lasting impact of neonatal Abx administration on the MGB axis, specifically on

*Corresponding author at: Department of Anatomy, Physiology and Cell Biology, School of Veterinary Medicine, University of California Davis, One Shield Avenue, Davis, CA, USA., mgareau@ucdavis.edu (M.G. Gareau).

[1]Authors contributed equally.

[2]Current address: Eurecat, Centre Tecnològic de Catalunya, Unitat de Nutrició i Salut, Reus, Spain.

Appendix A. Supplementary data

Supplementary data to this article can be found online at https://doi.org/10.1016/j.bbi.2020.11.001.

myelin regulation in the PFC region, potentially contributing to impaired cognitive function and bacterial metabolites are effective in reversing this altered phenotype.

1. Introduction

In recent years it has become increasingly evident that components of the gut microbiota are crucial for the correct development of the brain, gut, and immune system (Cryan et al., 2019; Ntranos and Casaccia, 2018; Round and Mazmanian, 2009). Alterations to the gut microbiota are increasingly being identified in patients with both gastrointestinal (GI) disease, including inflammatory bowel diseases (IBD) and irritable bowel syndrome (IBS), as well as psychological diseases, including major depressive disorder (MDD), and autism spectrum disorders (ASD) (Cryan et al., 2019; Ghaisas et al., 2016; Kho and Lal, 2018; Round and Mazmanian, 2009). Since colonization of the GI tract, formation of the GI mucosal barrier, and neural development in the brain all occur during a critical window in early neonatal life (Arrieta et al., 2014; Cryan et al., 2019; Derrien et al., 2019), exposure to events that can induce dysbiosis, such as stress or infection during neonatal life could detrimentally impact the establishment of the microbiota, gut, and brain (MGB) axis (Arrieta et al., 2014; Cotten, 2016; Cowan et al., 2019; Cryan et al., 2019).

While the gut and brain are distant organs, their connection via the nervous and immune systems offers multiple potential pathways by which communication can occur (Carabotti et al., 2015; Yoo and Mazmanian, 2017). Nerves in particular, with their rapid ability to signal to distant sites, represent a likely pathway through which the gut can signal to the brain. Myelin is a principal regulator of axonal conduction within the central nervous system (CNS), critical for regulating motor, sensory, and cognitive functions (Gacias et al., 2016; Hoban et al., 2016; Ntranos and Casaccia, 2018; Sharon et al., 2016). Myelination in the CNS is dependent on specialized glial cells known as oligodendrocytes, which are responsible for the dynamic integration of neurons and construction of the myelin lipid bilayer (Ntranos and Casaccia, 2018; Sharon et al., 2016). At birth, humans are born with mostly unmyelinated axons, with rapid myelination occurring in the few years after birth by oligodendrocytes (Oligodendrocyte transcription factor 2 [Olig2] expressing cells) (Lu et al., 2002; Williamson and Lyons, 2018). Although the total myelin content and rate of myelination is variable over time (Benes, 1989), myelination continues into the fourth decade of life (Lebel et al., 2012) in an organized spatiotemporal manner to maintain efficient proper circuit conduction. Given that the extent of myelination is correlated with brain plasticity and function, regulation of myelination is critical (Almeida and Lyons, 2017; Kaller et al., 2017; Williamson and Lyons, 2018).

As myelin abnormalities can detrimentally impact brain function, the role of myelination in cognitive function has been well studied (Gacias et al., 2016; Hoban et al., 2016; Ntranos and Casaccia, 2018). The prefrontal cortex (PFC) region in particular is an area that exhibits later myelination, during early neonatal life, making it more susceptible to external influences, such as intestinal dysbiosis (Hoban et al., 2016). The PFC region is also a key brain region implicated in numerous neuropsychiatric disorders, including MDD and ASD, both of which have increasing evidence of gut dysbiosis associated with disease

development (Goto et al., 2010; Hoban et al., 2016). Recently, it was established through the use of germ-free (GF) mice that the microbiota is necessary for myelination and maintaining of myelin plasticity (Hoban et al., 2016). Dysregulated myelination in the PFC detrimentally affected social behavior in mice following fecal transplantation in GF mouse studies (Gacias et al., 2016; Hoban et al., 2016; Sharon et al., 2016), although a mechanism outlining the role of the gut microbiota in these studies was not established. It has been demonstrated that bacterial metabolites, short chain fatty acids (SCFAs), can beneficially impact stress-induced behavioral deficits and intestinal barrier dysfunctions (van de Wouw et al., 2018), and can regulate myelination within the PFC region of the brain (Gacias et al., 2016) suggesting a novel MGB axis pathway.

Given the ability of Abx administration in mice to detrimentally impact the gut microbiota, impair myelination of PFC region neurons, and the ability for myelination in the PFC to continue into adulthood, we hypothesized that administration of Abx in neonatal life could impact the development of the MGB axis via altered myelination in the PFC region. Herein we demonstrate that neonatal Abx administration disrupts the developing MGB axis, via alterations in myelination within the PFC, which can be restored by oral administration of the beneficial bacterial SCFA butyrate.

2. Methods

2.1. Animals

Adult (6–8 weeks of age) male and female wild-type C57BL/6J (Jackson Labs, bred in-house) mice in equal numbers were utilized for the study. Mice were group-housed in cages (4 mice per cage), lined with chip bedding, and had access to food (standard chow) and water *ad libitum* throughout the study. The vivarium lighting schedule maintained 12 h of light and 12 h of darkness each day with the temperature set to 21 ± 1 °C. During treatment, mice were monitored daily for health status. No adverse events were observed throughout the experimental study. The experimenters were blinded to the pharmacological treatment while processing samples. Mice were euthanized by CO_2 asphyxiation followed by cervical dislocation or isoflurane inhalation followed by perfusion with 4% paraformaldehyde (PFA) for imaging studies. All procedures and protocols were reviewed and approved by the Institutional Animal Care and Use Committee at the University of California, Davis (IACUC #20072).

2.2. Abx administration

Entire litters of C57BL/6J mice (dam + pups) were randomized for Abx treatment or vehicle control for a period of 16 days starting from postnatal day (P) 7 to post-weaning (P23). An Abx cocktail consisting of vancomycin (0.5 mg/ml), neomycin (1 mg/ml), and ampicillin (1 mg/ml) was administered in drinking water (dam) and *via* oral gavage (litter: 50 μl per pup; between 9 and 11am). Control mice were gavaged daily with vehicle (water). Abx were chosen because they are poorly absorbed systemically and often administered in combination to deplete the microbiota (Frohlich et al., 2016). Dams were provided the Abx cocktail *ad libitum* in the drinking water to mitigate effects of coprophagy on the microbiota in older pups. A cage change was performed 48 h post initiation of Abx treatment to avoid

coprophagy by the dam impacting the microbiota. Mice were weaned at P21 and Abx continued in the drinking water for 48 h after weaning to ensure dysbiosis was maintained throughout the transitional period of weaning (P21). Both Abx-treated and control mice were provided normal water from P23 until adulthood (6–8 weeks of age) and each litter divided into experimental groups described in the Study Design (described below) to reduce any litter effects.

2.3. Study design

Adult mice were separated into 3 groups: (1) behavior, (2) intestinal physiology or (3) immunofluorescence (Fig. 1) with male and female mice distributed evenly. Mice in group #1 were euthanized after completion of behavioral testing. Additional tissues from these mice were collected for qPCR, western blot, and fecal pellets were collected for 16S Illumina sequencing and analysis of SCFA by Liquid Chromatography-mass spectrometry (LC-MS). Mice in group #2 were euthanized and ileal tissue was immediately mounted on Ussing chambers in order to assess intestinal physiology. Mice in group #3 were anesthetized with 5% isoflurane and transcardially perfused with 4% PFA for imaging studies.

2.4. Microbiota analysis

Colonic fecal pellets (N = 6 males and 6 females; 2 pellets per mouse; 2 mice per cage) were collected and snap-frozen with liquid nitrogen. DNA was extracted using the PowerFecal kit (Qiagen) by the UC Davis Host Microbe Systems Biology core and sample libraries were prepared and analyzed by barcoded amplicon sequencing. In brief, the purified DNA was amplified on the V4 region of the 16S rRNA genes via PCR using the following primers: F319 (5′-ACTCCTACGGGAGGCAGCAGT-3′) and R806 (5′-GGACTACNVGGGTWTCTAAT-3′). High-throughput sequencing was performed with Illumina MiSeq paired end 250-bp run. Raw sequences have been uploaded to the SRA (Sequence Read Archive) under accession SRP188244. Raw sequences were previously analyzed by sex (Pusceddu et al., 2019b).

The data derived from sequencing was processed by the UC Davis Mouse Metabolic Phenotyping Core (MMPC) using QIIME2 for 16S based microbiota analyses (Bolyen et al., 2019). Demultiplexed paired end sequences that already had barcodes and adapters removed were analyzed using Qiime 2 version 2018.4. For quality filtering and feature (OTU) prediction, we used DADA2 (Callahan et al., 2016). Forward reads were truncated to 270 nts and reverse reads to 220 nts. Representative sequences were aligned using MAFFT (Katoh and Standley, 2013). A phylogenetic tree of the aligned sequences was made using FastTree 2 (Price et al., 2010). OTUs/features were taxonomically classified using a pre-trained Naive Bayes taxonomy classifier. The classifier was trained using the Silva 128 97% OTUs (Quast et al., 2013) for the 319F-806R region. Diversity analyses were run on the resulting OTU/feature tables to provide both phylogenetic and non-phylogenetic metrics of alpha and beta diversity (Lozupone et al., 2011). Kruskal Wallis pairwise comparisons were used to statistically compare the alpha diversity measures and PERMANOVA was used for beta diversity. A multivariate statistical approach, Analysis of Composition of Microbiomes

(ANCOM), was used to compare the bacterial community at both phylum and family level using sex as a covariate (Mandal et al., 2015).

2.5. Ussing chambers

Distal ileum was collected and cut along the mesenteric border and mounted in Ussing chambers (Physiologic Instruments, San Diego, CA), exposing 0.1 cm^2 of tissue to 4 ml of circulating oxygenated Ringer's buffer maintained at 37 °C. The Ringer's buffer consisted of 115 mM NaCl, 1.25 mM $CaCl_2$, 1.2 mM $MgCl_2$, 2.0 mM KH_2PO_4 and 25 mM $NaHCO_3$ at pH 7.35 ± 0.02. 10 mM glucose was added to the serosal side as a source of energy, which was counterbalanced osmotically with 10 mM mannitol on the mucosal side. Agar–salt bridges were used to monitor potential differences across the tissue and served to inject the required short-circuit current (I_{sc}) necessary to maintain the potential difference at zero, registered by an automated voltage clamp. A computer connected to the voltage clamp system recorded I_{sc} continuously using acquisition software (Acquire and Analyze, Physiologic Instruments). Baseline I_{sc} values were obtained at equilibrium, ~15 min after the tissues were mounted onto the chamber. Isc, an indicator of active ion transport, was expressed in μA/cm^2. Intestinal permeability was assessed by measuring baseline conductance (G) for tight junction permeability as calculated from the inverse of resistance (1/R) using V = IR. The flux of FITC-labeled dextran (FD4, Sigma) was assessed over time (sampling every 30 min for 2 h) to measure macromolecular permeability. After 2 h, tissues were treated with forskolin (FSK, 20 uM; a cAMP agonist) to confirm tissue viability following completion of the experiment.

2.6. Behavioral tests

Behavioral tests were performed in a single day as previously described (Pusceddu et al., 2019a) from least to most stressful: Light/dark (L/D) box test, open field test (OFT) and finally novel object recognition task (Crawley, 2008). The sequence for behavioral tests has been demonstrated to prevent carry-over between tests (Pusceddu et al., 2019a). Behavioral testing was performed and analyzed in a blinded manner by two separate investigators (MP and JS) to avoid any bias and increase robustness of the data.

2.6.1. L/D box—To measure anxiety-like behavior, the L/D box test was used as described previously (Gareau et al., 2011). Briefly, mice were placed in a box with a light (2/3) and a dark (1/3) compartment and allowed to explore for 10 min. The time spent in the light box and the number of times the mouse transitioned from the dark compartment to the light compartment of the box were quantified via digital tracking system (Ethovision).

2.6.2. OFT—General locomotor activity was tested using the OFT. Behavior was recorded for 10 min in the novel arena (30 × 30 cm white plexiglass box) during acclimation for the novel object recognition (NOR) task. Both locomotor activity and anxiety-like behavior were determined as quantification of total distance traveled, time spent in the inner zone, and frequency of inner zone entries as analyzed by a digital tracking system (Ethovision).

2.6.3. NOR task—The NOR task was performed as previously described (Pusceddu et al., 2019a). Briefly, mice were subjected to 10 min of acclimation (served as the OFT) to the novel arena (30 × 30 cm white plexiglass box) followed by 5 min of exploration of two identical objects (training phase). After a rest and recovery period (45 min) one of the two original objects was replaced with a novel object and interactions were monitored for an additional 5 min (testing phase). Direct contact with nose (within 1–2 cm of the object) was recorded and scored manually and using Ethovision (XT 8.5, Noldus, Leesburg, VA) and verified manually. Mice that were not directly interacting with the object but rather exploring the chamber were not interpreted as direct contact with the object and omitted. Results were expressed as a ratio (exploration ratio) quantifying preference for exploration of a novel object rather than a familiar object during the testing phase. An exploration ratio of greater than 50% indicated that the mouse investigated the novel object more than the familiar object, showing memory recall for the latter. Mice that did not pass the training phase (<40% or greater than 60% exploration ratio which suggested a bias towards one object) or mice that did not explore the objects a total of 10 times were omitted.

2.7. qPCR

Tissues (PFC, hippocampus, ileum) were collected and frozen at —80 °C in Trizol (Invitrogen). RNA was isolated according to the manufacturer's protocol (Invitrogen), treated with DNase 1 (Invitrogen) and cDNA synthesized (iSCRIPT cDNA Synthesis Kit [Bio-Rad]). qPCR was performed using SYBR green on a QuantStudio 6 Flex Real-time PCR machine (Applied Biosystem). β-actin was used as a housekeeping gene and data were analyzed using the $2^{-\Delta\Delta CT}$ method to calculate the relative fold gene expression of each tissue sample to β-actin. All primer sequences used in this study are provided in Table 1.

2.8. Immunofluorescence

Mice were anesthetized (5% isoflurane) and transcardially perfused with PBS followed by 4% PFA. Brains were post-fixed in PFA overnight at 4 °C and cryoprotected in sucrose (30% sucrose (w/v) + 0.1% NaAz (v/v)) for 4 days before embedding in optimal cutting temperature (OCT) medium in ice-cold isopentane. OCT embedded brains were stored at least 48 h at –80 °C before cutting. PFC and hippocampus regions of the brain were cut using a cryostat (Leica Microsystems, Germany) into 20 μm-thick coronal sections. Sections were serially collected onto positively charged glass slides and stored at –20 °C until use. Immunofluorescence was performed as previously described (Pusceddu et al., 2019a). Briefly, sections underwent an antigen retrieval step using citrate buffer (10 mM, pH 6.0, 1 h, 95 °C). After blocking in 5% BSA normal goat serum (1 h, RT), samples were incubated with primary antibody overnight (16 h, 4 °C). Slides were washed (3 × 5 min) and incubated with appropriate secondary antibodies for 1 h at RT. Slides were washed once more and nuclei stained with DAPI. Slides were mounted in Prolong diamond (Invitrogen) for image analysis. Rabbit anti-Ki67 (LS-C141898, Lifespan Biosciences, Seattle, WA; RRID: AB_10949379), guinea pig anti-DCX (AB2253, Millipore, Burlington, MA; RRID: AB_1586992), rabbit anti-Sox10 (#89356, Cell Signaling Technology, USA; RRID:AB_2792980), rabbit anti-Olig2 (#AB9610, Millipore, USA; RRID: AB_570666), and mouse anti-MBP (#808401, BioLegend, USA; RRID:AB_2564741) were used as primary antibodies. Secondary antibodies include Alexa 647 goat anti-rabbit (Ab150155,

Abcam, Cambridge, UK), Alexa 555 goat anti-guinea pig (A21435, Invitrogen). For SOX10 and OLIG2 co-staining and MBP staining, Zenon™ Alexa Fluor™ 555 Rabbit IgG Labeling Kit (Invitrogen) and Zenon™ Alexa Fluor™ 647 Rabbit IgG Labeling Kit (Invitrogen) were used according to the manufacturer instructions. Nuclei were stained with DAPI, followed by 4% PFA cell fixation step. Slides were mounted in Prolong gold (Invitrogen) for image analysis.

2.9. Image analysis and cell quantification

Confocal imaging was performed on a Leica SP8 STED 3X microscope. Immunofluorescent Z-stack images were collected using a 20x objective with a 1.04 μm step size and a 63x objective with a 0.3 μm step size for the hippocampus and PFC, respectively. Systematic random sampling was used for the dorsal hippocampus by counting the cells in both hemispheres of each section in 1:6 series (120 μm apart). Every second section, for a total of three sections, was used for DCX/Ki67 co-staining [dentate gyrus (DG) area]. Cell quantification was performed using the image processing software package Imaris (x64_8.2.1). All cell numbers are expressed as counts averaged from 3 sections per animal. The dorsal hippocampus was defined as AP –0.94 to –2.30 according to the Paxinos and Franklin atlas of the mouse brain. For imaging Olig2/Sox10 co-staining, SOX10 mono-staining and MBP staining, medial-PFC region was taken in both hemispheres using a 40x/63x objective with a 0.35 μm and 0.3 μm step size, respectively. The medial-PFC region was defined as Bregma 1.94 to 2.10 mm according to the Paxinos and Franklin atlas of the mouse brain. IF for SOX10 was analyzed by calculating the number of SOX10-positive cells against DAPI-positive cells. Mean intensity fluorescence was calculated for MBP, using FIJI program.

2.10. Western Blot

Tissue was collected and snap frozen in liquid nitrogen before storing at –80 °C. Tissue was homogenized in RIPA buffer (Thermo Scientific) and protein concentration was measured using Bicinchoninic Acid (BCA) protein quantification assay (Bio-rad). Samples were diluted in 4x Laemmli SDS sample buffer (Bio-rad) and boiled for ten minutes before loading onto 10% Mini-Protean TGX precast gels (Biorad) for SDS-PAGE alongside a molecular weight ladder (PageRuler Pre-stained ladder, Thermo Scientific #26626). Gels were run in a Bio-Rad Mini-PROTEAN Tetra system at 120 V in Tris/Gycine/SDS buffer (Bio-rad). SDS-PAGE gels were transferred onto PVDF membrane (Bio-rad) in transfer Buffer (0.2 M Glycine, 24 mM Tris, 20% Methanol) at 100 V for 80 min. Protein was visualized on the membrane post-transfer using Ponceau S solution (Sigma Aldrich, #P7170). Membranes were blocked in 5% milk (w/v) in TB ST (50 mM Tris, 150 mM NaCl, 1% Tween) for 1 h at RT. Subsequently, membranes were incubated with rabbit anti-Sox 10 (Abcam #ab155279; RRID: AB_2650603), rabbit anti-MYRF (Millipore #ABN45; RRID: AB_2750648) or rabbit anti-βactin (Santa Cruz #sc-16161; RRID: AB_630836) at 4 °C O/N. The following day, membranes were washed in TB ST and incubated with secondary antibody (anti-rabbit, CST #7074S) for 1 h at RT. Membranes were washed a second time before being incubated with ECL western blotting substrate (Pierce). Membranes were imaged using Bio-rad Image lab. Proteins were stripped before re-probing with a new

antibody. For densitometric analysis, pixel intensities were measured using ImageJ and normalized to βactin.

2.11. Mass spectrometry

Fresh fecal samples from mice were collected and stored at –80 °C until analysis. Pellets were extracted with nano-pure water (10 mg/mL) and gently agitated overnight at 4 °C. The homogenized samples were centrifuged (21,000 g; 5 min) and supernatants (100 μl) transferred and centrifuged (21,000 g; 20 min). For each sample, 20 μl of the supernatant was mixed with 20 μl of 100 mM N-(3-Dimethylaminopropyl)-N0-ethylcarbodiimide hydrochloride (1-EDC HCl) in 5% pyridine and 40 μl of 200 mM 2-Nitrophenylhydrazine (2-NPH) in 80% acetonitrile (ACN) with 50 mM HCl (all chemical from Sigma-Aldrich). The mixture was incubated (40 °C; 30 min) and the reaction was terminated by ACN (10%; 400 μl). Samples were transferred to polypropylene vials and 1 μl of the solution was injected into an Agilent 6490 triple quadruple mass spectrometer for analysis. Chromatographic separations were carried out on an Agilent C18 stationary phase (2.1 × 50 mm, 1.8 um) column. Mobile phases were 100% ACN (B) and water with 10% ACN (A). The analytical gradient was as follows: time = 0 min, 10% B; time = 4.5 min, 10% B; time = 10 min, 35% B; time = 10.1 min, 85% B; time = 11.6 min, 90% B; time = 12 min, 90% B. Flow rate was 0.3 ml/min and injection volume was 1 μl. Samples were held at 4 °C in the autosampler, and the column was operated at 40 °C. The MS was operated in selected reaction monitoring mode, positive ionization mode, and parameters were optimized with SCFA standards. The capillary voltage was set to 1.8 kV, source temperature was 200 °C and sheath gas temperature 200 °C. Gas flow was 11 L/min, sheath gas flow was 7 L/min, and collision gas flow was 0.2 ml/min. Nebulizer pressure (nitrogen) was set to 25 psi. Argon was used as the collision gas. A calibration curve was generated using SCFA standards.

2.12. Tributyrin administration

Mice were administered 10 mM tributyrin (or vehicle [water]) via oral gavage from P21 (weaning) to P23. Subsequently, 10 mM tributyrin was administered in the drinking water *ad libidum* until adulthood (6–8 weeks of age). Tributyrin was chosen over butyrate as it has a more palatable taste to mice and it has been demonstrated as an effective method for delivering butyrate to the intestine (Donovan et al., 2017).

2.13. Statistical analysis

Data sets were within normal distribution as demonstrated using D'Agostino-Pearson omnibus normality test (GraphPad Software Prism 8) prior to analyzing data via unpaired two-tailed Student's *t*-test (parametric data) or Mann-Whitney test (non-parametric data) as appropriate (GraphPad). Kruskal-Wallis was used for analysis of the microbiota (β-diversity) with p values corrected for multiple comparisons. Data was expressed as standard error of the mean (SEM), and values with $p < 0.05$ were considered statistically significant.

3. Results

3.1. Neonatal Abx administration leads to long-lasting gut dysbiosis

Bacterial community analysis was performed by 16S Illumina sequencing on fecal samples from neonatally Abx-treated and sham-treated mice at 4 weeks post-Abx treatment to identify long lasting impairments in the microbiota in adult mice. As previously reported (Cho et al., 2012), neonatal Abx administration led to significant changes in bacterial communities compared to sham-treated mice in adulthood, identifying a long-lasting impact of Abx on the microbiota. Kruskal-Wallis pairwise comparisons of the alpha-diversity metrics including Shannon and Simpson's indices were significantly lower ($p < 0.05$) in the neonatal Abx-treated group, indicating less diverse bacterial community within Abx samples compared to sham controls (Fig. 2A). Phylogenetic (unweighted and weighted UniFrac) and non-phylogenetic (Bray-Curtis and Jaccard) beta-diversity indices analyzed via PERMANOVA pairwise comparisons confirmed the presence of ongoing bacterial community shifts in adult mice following neonatal Abx administration, which suggests significant dissimilarity between the two groups (Fig. 2B). At the phylum level, ratio of Bacteroides:Firmicutes shifted following neonatal Abx administration, with Bacteroides abundance decreasing (35% to 14%) and Firmicutes abundance increasing (60% to 80%; Fig. 2C). The relative abundance of Actinobacteria decreased in adult mice following neonatal Abx administration, to almost undetectable levels (Fig. 2C). Proteobacteria and Tenericutes together accounted for<1% of the bacterial community in sham-treated mice; however, following neonatal Abx administration, their relative abundance increased to 1.65% and 5% respectively, in adult mice.

At the family level, more detailed changes in the bacterial community in two groups were identified. ANCOM scores revealed 12 families that were differentially abundant in sham vs. Abx-treated groups. The families of Alcaligenaceae, Bacteroidaceae, Coriobacteriaceae, Rikenellaceae, Family XIII, uncultured Firmicutes bacterium and Clostridiales were not detected in neonatal Abx-treated mice, in contrast to sham-treated controls (Fig. 2D). The relative abundance of Erysipelotrichaceae (6.75 ± 0.87 sham vs. 27.48 ± 9.61 Abx) and Paenibacillaceae (0 ± 0 sham vs. 18.48 ± 7.46 Abx), were significantly increased in adult mice following neonatal Abx-treatment. In addition, the relative abundance of Bacteroidales S24–7 group decreased to 13.79% in Abx-treated mice from 32.12% in sham-treated controls. Taken together, neonatal Abx administration causes long-term changes in the gut bacterial community, which persisted into adulthood.

3.2. Neonatal Abx administration alters ileal physiology without causing inflammation

Given previous findings of Abx-induced dysregulation in intestinal homeostasis (Pusceddu et al., 2019b; Rao et al., 2015), we assessed ileal physiology following neonatal Abx administration in mice using Ussing chambers. Ileal physiology was significantly impaired following neonatal Abx-treatment as determine by baseline Isc, indicating increased active ion transport compared to sham-treated controls (Fig. 3A). Paracellular tight junction permeability was assessed by measuring ileal conductance (G), demonstrating a significant increase in neonatal Abx-treated mice compared to sham-treated controls (Fig. 3B). Macromolecular permeability was assessed by measuring the flux of FITC-labeled dextran

in the serosal compartment, with increased FITC demonstrating increased ileal permeability in the neonatal Abx-treated mice compared to sham-treated controls (Fig. 3C). As increased gut permeability is known to trigger intestinal inflammation, we quantified gene expression levels of pro-inflammatory cytokines, innate immune markers, and pattern recognition receptors (*Ifnγ, Il1β, Il6, Tnfα, RegIIIγ, IκBα, Nod1, Nod2, Tlr2, Tlr4, Tlr6, Tlr9*) in the ileum, as well as the anti-inflammatory cytokine *Il10*. Despite the changes seen in ileal physiology by Ussing chambers, neonatally Abx-induced dysbiosis was associated with decreased *Tnfα* and *Il10* expression, coupled with decreased expression of *Tlr2, 4, 6*, and *9* (Fig. 3D). This dampened innate immune response was largely absent at weaning, with only decreased expression of *RegIIIγ* and increased expression of *Tlr9* observed (Suppl Fig. 1A). Taken together, these findings suggest that altered host-microbe interactions result in impaired intestinal physiology and dampened innate immunity following neonatal Abx administration.

3.3. Neonatal Abx administration results in alterations in cognition and anxiety-like behavior in adulthood

Behavioral tests were performed to assess the effect of neonatal Abx administration on cognition, anxiety-like behavior, and general locomotor activity. Using the NOR task, neonatal Abx-treated mice exhibited significantly lower exploration ratio than sham controls, indicating a cognitive deficit (Fig. 4A). Anxiety-like behavior was assessed using both the L/D box test and OFT. Increased time spent in the light box during the L/D box test and increased time spent in the inner zone of the OFT compared to sham mice were observed, indicating anxiolytic behavior in neonatally Abx-treated mice (Fig. 4B–C). In contrast, locomotor activity showed no significant differences between Abx and sham groups in terms of total distance traveled and frequency of transition between the light and the dark boxes of the L/D box test and the inner and outer zone of the OFT (Fig. 4B–C). These data were congruent among sex, suggesting absence of any sexually dimorphic effects. Therefore, neonatal Abx administration resulted in cognitive deficits and anxiolytic behavior in adulthood.

3.4. Neonatal Abx administration leads to myelin dysregulation in the brain in adulthood

Given the role of myelin on memory formation and cognitive function, assessment of myelin-related genes was performed by qPCR in the PFC region and hippocampus. Upregulation of myelin related genes (myelin-associated glycoprotein; *Mag,* myelin oligodendrocyte glycoprotein; *Mog,* myelin-associated oligodendrocytic basic protein; *Mobp*, and proteolipid protein; *Plp*) was demonstrated in the PFC region of neonatal Abx-treated mice compared to sham-treated controls (Fig. 4D). In the hippocampus, similar increases in gene expression of *Mag, Mog,* and *Plp* were found, but there was no change in expression of *Mbp* and *Mobp* in the Abx-treated group (Fig. 4E). Together, these findings suggest that neonatal Abx administration leads to increase in myelin-related gene expression in the PFC region. To assess whether changes in myelin-related genes led to changes in myelin, myelin basic protein (MBP) was quantified. Expression of *Mbp* was significantly increased in the PFC of Abx-treated mice. Subsequently, immunofluorescence for MBP was performed and the mean fluorescence intensity (MFI) quantified. MBP expression was significantly increased in Abx-treated mice, suggesting presence of more myelin in the PFC

region (Fig. 4F). To further verify the effect on oligodendrocyte development and myelination induced by neonatal Abx, we assessed the same set of myelin-related genes in the PFC and the hippocampus in mice at age of P21. Abx-treated mice did not show increased expression of myelin-associated genes in both of the brain regions compared to the sham-treated mice, suggesting the alterations of myelination begin to emerge following weaning with impairments identified in adulthood. (Suppl Fig. 1B–C).

3.5. Neonatal Abx administration leads to differentiation and maturation of oligodendrocytes

Myelin-associated genes (*Mag, Mog, Mbp, Mobp, Plp*) and transcription factors *Sox10* and *Myrf* (sry-related high mobility-box transcriptional regulator; [*Sox10*] and myelin regulatory factor [*Myrf*]) are lineage-specific of oligodendrocyte maturation and expression of these genes can be an indicator for the specific developmental stage of the oligodendrocytes (Mitew et al., 2014). Since these genes and transcription factors were upregulated in the PFC region following neonatal Abx administration, we assessed gene expression for pre- and mature myelinating oligodendrocytes, as well as oligodendrocyte precursor cells (OPCs) to identify impairments in oligodendrocyte maturation in sham and Abx-treated mice. OLIG2, SOX10, PDGFRα, and CNPase were used to classify oligodendrocyte lineage. Gene expression levels of *Pdgfra* were significantly downregulated in the PFC region of neonatally Abx-treated mice, whereas *Cnp* was significantly upregulated compared to the sham-treated mice suggesting the presence of increased numbers of myelinating oligodendrocytes (Fig. 5A). Increases in *Olig2* expression in neonatally Abx-treated mice suggested a higher abundance of oligodendrocytes compared to sham-treated mice in the PFC region (Fig. 5A). Confocal imaging of SOX10 and OLIG2 expression in the medial PFC region was performed to assess protein expression. Both sham- and Abx-treated groups showed co-localization of SOX10 and OLIG2, however, expression of SOX10 was significantly increased in neonatally Abx-treated mice compared to sham-treated controls, supporting the gene expression studies (Fig. 5B). SOX10 and MYRF were both quantified by western blot, which identified increases in mice neonatally-treated with Abx (Fig. 5C). Thus, neonatal Abx administration appears to increase maturation of OPCs in the PFC region and increase the production of myelin.

3.6. Neonatal Abx administration impairs hippocampal neurogenesis

Given that cognitive function is associated with neurogenesis in humans (Hill et al., 2019), and that myelin is critical for maturation and stabilization of neurons, we assessed whether neurogenesis was impacted following neonatal Abx administration via qPCR for *Bdnf* gene expression and immunofluorescence of DCX and Ki67 in the proliferative zones of the hippocampus (Bordiuk et al., 2014). A decrease in *Bdnf*, a key regulator of neurogenesis, was observed in neonatally Abx-treated mice versus sham-treated controls (Fig. 6A). Additionally, a decrease in immature neurons was identified in neonatally Abx-treated mice, as evidenced by decreased numbers of DCX positive cells in the proliferating DG region of the hippocampus, however there was no significant difference in the total number of proliferating cells, as determined by Ki67 staining (Fig. 6B). Thus, neonatal Abx administration can impair hippocampal neurogenesis in adulthood.

3.7. Tributyrin supplementation rescues behavioral deficits, intestinal pathophysiology, and myelin dysregulation in adulthood following neonatal Abx administration

SCFAs are important for maintaining intestinal health (Makki et al., 2018; Morrison and Preston, 2016) and have recently been shown to also beneficially modulate brain function and behavior (van de Wouw et al., 2018). Given that altered SFCA levels are associated with alterations in the gut microbiota, coupled with the persistent dysbiosis seen in adult mice following neonatal Abx administration, fecal SCFA levels were quantified. Neonatally Abx-treated mice had decreased fecal levels of multiple SCFAs including glyceric acid, lactic acid, acetic acid, propionic acid, and butyric acid compared to sham-treated mice (Fig. 7A). Butyrate in particular is an important SCFA produced by the microbiota that has been shown to be beneficial in improving intestinal physiology, including ion transport and tight junction permeability, following Abx treatment (Cresci et al., 2013). We hypothesized that restoring decreased levels of butyrate caused by neonatal Abx administration we might rescue the detrimental effects of Abx administration in the gut and brain. Mice were therefore treated with tributyrin (Tb) daily for 4 weeks starting at weaning (P21).

Ussing chamber studies revealed that Tb administration prevented elevated Isc and G in Abx-treated mice, however FITC flux remained elevated (Fig. 7B) This may be due in part to the ability of Tb administration to significantly improve barrier function in sham mice (Sham: 887.1 ± 112.6 vs. Sham + Tb: 445.8 ± 131.6 ng/cm^2/hr).

In the NOR task, Abx + Tb mice displayed similar recognition ratios to Sham + Tb mice, suggesting Tb could rescue the Abx-induced cognitive deficit (Fig. 7C). In the L/D box, the time spent in the light and transitions were similar between the Abx Tb and Sham Tb mice (Fig. 7D). In the OFT, Abx + Tb mice travelled a similar distance and spent similar time in the inner zone compared to Sham + Tb mice (Fig. 7E) supporting the L/D box findings. Taken together, both cognitive behavioral deficits and anxiolytic behaviors were prevented by Tb administration.

Along with the improvements in behavior, expression of myelin-associated genes and IGF signaling molecules in the PFC were quantified. Expression of *Mag, Mog, Mbp, Mobp, Myrf,* and *Sox10* was normalized to levels seen in sham-treated controls, with an exception of *Plp1,* which was significantly downregulated in the Abx + Tb compared to Sham + Tb mice (Fig. 7F) suggesting Tb prevented deficits in myelin gene expression induced by neonatal Abx administration. Furthermore, protein expression of SOX10, MYRF, and MBP in the PFC was similar in both Abx + Tb and Sham + Tb mice (Fig. 7G–H). Finally, hippocampal *Bdnf* expression was restored (Fig. 7J) suggesting normalization of Abx-induced impaired neurogenesis by tributyrin administration. Interestingly, Tb supplementation did not increase butyric acid levels in either the cecum or in fecal pellets, with levels in supplemented mice decreased in both compartments compared to sham treated controls and not restored in Abx + Tb treated mice (Table 2).

4. Discussion

Bidirectional communication between the gut and the brain can be influenced by both environmental and dietary stimuli, altering the gut microbiota and impacting the immune

system (Cryan et al., 2019; Sharon et al., 2016; Yoo and Mazmanian, 2017). Establishment of the MGB axis starts at birth, beginning with colonization of the gut microbiota, and rapidly developing during the early stages of life (Arrieta et al., 2014; Derrien et al., 2019). Therefore, exposure to harmful stimuli can potentially impede this delicate balance of developmental processes, leading to an impaired immune system, altered behavior, and ultimately neurodevelopmental disorders. One potential mechanism through which the MGB axis may influence behavior and cognition is via myelination in the PFC, which integrates input from multiple brain regions to process complex decision-making and memory retrieval (Cowan et al., 2019; Gacias et al., 2016; Goto et al., 2010; Hoban et al., 2016; Kaller et al., 2017; Ntranos and Casaccia, 2018). Given that significant myelination occurs during neonatal life and continues until early adulthood (Kaller et al., 2017; Ntranos and Casaccia, 2018; Williamson and Lyons, 2018), coinciding with development of the MGB axis, alterations in this process may lead to long-term deficits. However, to our knowledge, the impact of myelin regulation following neonatal dysbiosis in adulthood remains unknown. Previously, Hoban et al. demonstrated the presence of hypermyelination in the PFC region of GF mice (Hoban et al., 2016). Here, for the first time, we show that neonatal Abx administration results in oligodendrocyte impairment and altered myelin in the PFC region, coupled with behavioral deficits, in the context of dysbiosis of the gut microbiota in adulthood, which could be prevented by SCFA supplementation.

The gut microbiota is important in maintaining neural development and myelination (Hoban et al., 2016; Rao et al., 2015), although exact mechanisms involved remain unknown. In the current study, nonabsorbable Abx were administered in early life to investigate a potential link between gut dysbiosis and myelination in the CNS. Neonatally Abx-treated mice exhibited altered gut microbiota colonization patterns in adulthood compared to sham-treated controls, as demonstrated by reduced beta-diversity. At the phylum level, an altered Bacteroides: Firmicutes ratio was coupled with decreased Actinobacteria and increased Proteobacteria, suggesting a potential increase in colonization of pathobionts. Firmicutes can have beneficial/protective effects on both cognitive function (Kaakoush, 2015) and GI physiology (Forbes et al., 2016; Huang et al., 2018) making them important in MGB axis signaling. Alterations in several families within the Firmicutes phylum, including absence of Lactobacillaceae and large increases in Erysipelotrichaceae, may have contributed to MGB axis deficits in Abx-treated mice. At the family level, 12 families were identified as being differentially abundant compared to sham controls. Paenibacillaceae, absent in sham-treated mice, was among the third most abundant family in Abx-treated mice, similar to findings from previous Abx studies (Grayson et al., 2018). Alcaligenaceae and Rikenellaceae families, which are increased in neurodegenerative diseases and cognitive impairments (Gomez-Hurtado et al., 2014; Ren et al., 2020), were significantly reduced in Abx-treated mice. Furthermore, Coriobacteriaceae, found to beneficially regulate the intestinal environment in marathon runners (Zhao et al., 2018) and is decreased in IBD patients (Pittayanon et al., 2020), was absent in Abx-treated mice, suggesting their absence may have contributed to the observed impairment in gut permeability. Additionally, neonatal Abx administration significantly decreased the relative abundance of Bacteroidales S24–7, a predominant family in mice, by almost half. While a clear function of Bacteroidales S24–7 in gut homeostasis remains unknown, it is thought to promote butyrate production (Ormerod

et al., 2016; Smith et al., 2019; Zhuang et al., 2019) and levels are depleted in chemically-induced colitis (Osaka et al., 2017). Bacteroidaceae, which is important for SCFA production, was also absent in the neonatal Abx treated group. Finally, the absence of Bacteroidaceae and Coriobacteriaceae, which are reduced in multiple sclerosis patients (Jangi et al., 2016; Yan and Charles, 2018), may also suggest a potential association between Abx-induced gut dysbiosis and altered myelination in the brain.

Administration of Abx occurs at a higher rate in children compared to adults, due to their increased risk of exposure to bacterial pathogens and their immature immune system (Arrieta et al., 2014; Cotten, 2016). In mouse models, Abx administration in adulthood (Desbonnet et al., 2014), adolescence (Leclercq et al., 2017), or maternal administration during gestation (Hornig et al., 2013) can cause impairments in behavior including cognitive dysfunction and anxiolytic behavior. These Abx-induced behavioral effects closely mimic those seen in GF mice (Cowan et al., 2019; Hoban et al., 2016). In our mouse model of neonatal administration of Abx, we found a persistent effect on behavior in adulthood, with cognitive deficits and anxiolytic behaviors. While behavioral impairments were observed in the absence of overt GI inflammation, a potentially impaired mucosal immune response was observed, with decreased cytokine and PRR expression identified. These increased ion transport and increased permeability were both identified in the ileum, suggesting that host-microbe interactions were impaired.

Given the role of myelin in maintaining cognitive function, we assessed expression of myelin and myelin-related genes in the hippocampus and PFC regions. Expression of myelin-related genes was dysregulated, with neonatally Abx-treated mice demonstrating higher expression of *Mag, Mog, Mbp, Mobp* and *Plp* in the PFC and increases in *Mag, Mog* and *Plp* in the hippocampus. As the transcription factors *Sox10* and *Myrf* were also significantly upregulated in the PFC of Abx-treated mice, these findings suggest alterations in differentiation of oligodendrocytes and the regulation of myelin-related gene expression in the PFC region. Furthermore, protein expression of SOX10, MYRF and MBP were significantly increased in the PFC of Abx-treated mice, corroborating long-lasting increased myelination effect post neonatal Abx administration. These findings are in line with Hoban et al., where GF mice displayed upregulation of myelin genes in the PFC region compared to conventionally colonized controls (Hoban et al., 2016). Additional electron microscopy or electrophysiology studies could yield further support for these findings, providing some structural insight into the impact of increased myelin on hippocampal axons. Thus, the long-lasting behavioral alterations identified following neonatal Abx administration may be correlated with myelin dysregulation in the PFC region.

Oligodendrocytes are derived from OPCs and are continuously generated throughout life, with rates declining in adulthood (Williamson and Lyons, 2018). Maturation of oligodendrocytes depends on lineage specific gene expression and protein translation. Oligodendrocyte-lineage specific genes, *Mag* and *CNPase*, are pre-myelinating genes whose expression initiates maturation of OPCs. In contrast, *Mbp, Mobp,* and *Mog* are only expressed in mature oligodendrocytes and are regulated by MYRF, which physically binds with SOX10 (Novotny et al., 2019). Here, Abx-treated mice displayed significant increases in all of these myelin-related genes, suggesting increased mature oligodendrocytes

producing myelin. This finding may indicate (1) delayed myelination due to neonatal dysbiosis with increases in myelinating oligodendrocytes trying to recover this process and/or (2) hyper myelination due to myelin dysregulation. These findings suggest that impacts on myelination induced in early life can be maintained well into adulthood.

Synaptic plasticity, neurogenesis, and myelin plasticity are thought to operate in a coordinated and synergistic manner to regulate neural networks and support functions such as learning and memory, which span multiple CNS regions including the hippocampus and PFC region (O'Rourke et al., 2014; Warburton and Brown, 2015). Impairments in hippocampal neurogenesis can therefore impact other regions, such as myelination in the PFC region. Cognitive function is thought to mainly involve the hippocampus and PFC regions although specific behaviors associated with each area remain controversial. An intricate neural circuit within specific structures of the brain, including the perirhinal cortex, the hippocampus, and the mPFC, is suggested to regulate processes of recognition memory associated to both objects and places (Norman and Eacott, 2004; Warburton and Brown, 2015). While a number of studies suggest an effect of hippocampal lesions in recognition memory (Clark et al., 2001, 2000), other studies do not (Good et al., 2007; Mumby et al., 2002). Decreased neurogenesis, coupled with decreased expression of the neurotrophic factor BDNF, together suggest a potential pathway through which impaired cognitive function was mediated. How and whether this is connected to the impaired myelin remains to be determined, but it suggests that the impacts of early life Abx may extend to long-lasting effects in the CNS. Future studies to ascertain which specific brain areas are predominantly involved in the Abx-induced cognitive alterations are highly warranted.

Butyrate is an important energy source for colonocytes produced by beneficial bacteria. Excess butyrate not utilized by the colon or liver can circulate to the CNS and positively regulate neurological effects (Bourassa et al., 2016), while oral butyrate administration can enhance CNS remyelination in mice (Chen et al., 2019). Decreased intestinal concentrations of SCFA are often found in disease models where dysbiosis is observed (Vieira et al., 2012). Interestingly, however, supplementation with SCFA, for example butyrate, often doesn't restore these intestinal levels despite improving disease outcomes (van de Wouw et al., 2018; Vieira et al., 2012). Given that neonatal Abx administration significantly reduced fecal butyrate levels, and the positive association between SCFA administration and behavior (van de Wouw et al., 2018), butyrate was administered to restore altered MGB signaling and myelination induced by neonatal Abx administration. Indeed, daily administration of tributyrin starting at weaning normalized intestinal physiology, with ion transport and tight junction permeability both restored to sham levels in the ileum. Macromolecular permeability was still enhanced, however this may in part be due to an improvement in permeability by tributyrin in the sham-treated group. In the NOR task, Abx + Tributyrin-treated mice performed similarly well to the Sham + Tb butyrin group, suggesting restoration of recognition memory. This beneficial effect of butyrate is consistent with previous findings, where butyrate supplementation ameliorated cognitive deficits in models of chronic stress or neurodegenerative disease, while not directly impacting butyrate levels within the fecal contents in the gut (Liu et al., 2015; Sharma et al., 2015; Stilling et al., 2016; van de Wouw et al., 2018). Similarly, anxiolytic behavior observed in Abx-treated mice was reduced by tributyrin administration, with mice performing similarly to the Sham

+ Tb in the L/D box task with respect to time spent in the light box and decreased time spent in the inner zone in the OFT. Tributyrin administration also normalized the myelin gene expression in the PFC of neonatally Abx-treated mice, with expression of myelin-related genes in the PFC similar to sham-treated mice. Taken together these data suggest that the microbiota and specific microbial metabolites such as butyrate can serve as a key regulators of myelin gene expression within the CNS and dysregulation of this pathway caused by dysbiosis can have long-lasting impacts on behavior in adulthood.

In conclusion, we propose for the first time that myelination can be chronically dysregulated throughout adult life following Abx-induced neonatal dysbiosis, resulting in cognitive and behavioral deficits. Tributyrin supplementation can reverse the impairment caused by Abx administration on myelination and behavior, identifying an important role for the neonatal microbiota in the establishment of myelination and signaling of the gut-brain axis. Future studies, such as a myelin-associated gene knockout mouse models, will be important to verify the exact function of the microbiota on myelin expression in the CNS that can play a crucial role in signaling of the MGB axis.

Supplementary Material

Refer to Web version on PubMed Central for supplementary material.

Acknowledgement

This research was supported by the NIH 1R01AT009365-01 (MGG) and NIH U24-DK092993 (UC Davis Mouse Metabolic Phenotyping Center (RRID:SCR_015361)).

Abbreviations:

Abx	antibiotics
L/D	light/dark
MGB	microbiota-gut-brain
NOR	novel object recognition
OFT	open field test
PFC	prefrontal cortex
SCFA	short-chain fatty acids
Tb	Tributyrin

References

Almeida RG, Lyons DA, 2017 On myelinated axon plasticity and neuronal circuit formation and function. J. Neurosci 37, 10023–10034. [PubMed: 29046438]

Arrieta MC, Stiemsma LT, Amenyogbe N, Brown EM, Finlay B, 2014 The intestinal microbiome in early life: health and disease. Front. Immunol 5, 427. [PubMed: 25250028]

Benes FM, 1989 Myelination of cortical-hippocampal relays during late adolescence. Schizophr. Bull 15, 585–593. [PubMed: 2623440]

Bolyen E, Rideout JR, Dillon MR, Bokulich NA, Abnet CC, Al-Ghalith GA, Alexander H, Alm EJ, Arumugam M, Asnicar F, Bai Y, Bisanz JE, Bittinger K, Brejnrod A, Brislawn CJ, Brown CT, Callahan BJ, Caraballo-Rodriguez AM, Chase J, Cope EK, Da Silva R, Diener C, Dorrestein PC, Douglas GM, Durall DM, Duvallet C, Edwardson CF, Ernst M, Estaki M, Fouquier J, Gauglitz JM, Gibbons SM, Gibson DL, Gonzalez A, Gorlick K, Guo J, Hillmann B, Holmes S, Holste H, Huttenhower C, Huttley GA, Janssen S, Jarmusch AK, Jiang L, Kaehler BD, Kang KB, Keefe CR, Keim P, Kelley ST, Knights D, Koester I, Kosciolek T, Kreps J, Langille MGI, Lee J, Ley R, Liu YX, Loftfield E, Lozupone C, Maher M, Marotz C, Martin BD, McDonald D, McIver LJ, Melnik AV, Metcalf JL, Morgan SC, Morton JT, Naimey AT, Navas-Molina JA, Nothias LF, Orchanian SB, Pearson T, Peoples SL, Petras D, Preuss ML, Pruesse E, Rasmussen LB, Rivers A, Robeson MS 2nd, Rosenthal P, Segata N, Shaffer M, Shiffer A, Sinha R, Song SJ, Spear JR, Swafford AD, Thompson LR, Torres PJ, Trinh P, Tripathi A, Turnbaugh PJ, Ul-Hasan S, van der Hooft JJJ, Vargas F, Vazquez-Baeza Y, Vogtmann E, von Hippel M, Walters W, Wan Y, Wang M, Warren J, Weber KC, Williamson CHD, Willis AD, Xu ZZ, Zaneveld JR, Zhang Y, Zhu Q, Knight R, Caporaso JG, 2019 Reproducible, interactive, scalable and extensible microbiome data science using QIIME 2. Nat. Biotechnol 37, 852–857. [PubMed: 31341288]

Bordiuk OL, Smith K, Morin PJ, Semenov MV, 2014 Cell proliferation and neurogenesis in adult mouse brain. PLoS ONE 9, e111453. [PubMed: 25375658]

Bourassa MW, Alim I, Bultman SJ, Ratan RR, 2016 Butyrate, neuroepigenetics and the gut microbiome: Can a high fiber diet improve brain health? Neurosci. Lett 625, 56–63. [PubMed: 26868600]

Callahan BJ, McMurdie PJ, Rosen MJ, Han AW, Johnson AJ, Holmes SP, 2016 DADA2: High-resolution sample inference from Illumina amplicon data. Nat. Methods 13, 581–583. [PubMed: 27214047]

Carabotti M, Scirocco A, Maselli MA, Severi C, 2015 The gut-brain axis: interactions between enteric microbiota, central and enteric nervous systems. Ann. Gastroenterol 28, 203–209. [PubMed: 25830558]

Chen T, Noto D, Hoshino Y, Mizuno M, Miyake S, 2019 Butyrate suppresses demyelination and enhances remyelination. J. Neuroinflamm 16, 165.

Cho I, Yamanishi S, Cox L, Methe BA, Zavadil J, Li K, Gao Z, Mahana D, Raju K, Teitler I, Li H, Alekseyenko AV, Blaser MJ, 2012 Antibiotics in early life alter the murine colonic microbiome and adiposity. Nature 488, 621–626. [PubMed: 22914093]

Clark RE, West AN, Zola SM, Squire LR, 2001 Rats with lesions of the hippocampus are impaired on the delayed nonmatching-to-sample task. Hippocampus 11, 176–186. [PubMed: 11345124]

Clark RE, Zola SM, Squire LR, 2000 Impaired recognition memory in rats after damage to the hippocampus. J. Neurosci 20, 8853–8860. [PubMed: 11102494]

Cotten CM, 2016 Adverse consequences of neonatal antibiotic exposure. Curr. Opin. Pediatr 28, 141–149. [PubMed: 26886785]

Cowan CSM, Dinan TG, Cryan JF, 2019 Annual Research Review: Critical windows – the microbiota-gut-brain axis in neurocognitive development. J. Child Psychol. Psychiatry

Crawley JN, 2008 Behavioral phenotyping strategies for mutant mice. Neuron 57, 809–818. [PubMed: 18367082]

Cresci G, Nagy LE, Ganapathy V, 2013 Lactobacillus GG and tributyrin supplementation reduce antibiotic-induced intestinal injury. JPEN J. Parenter. Enteral Nutr 37, 763–774. [PubMed: 23630018]

Cryan JF, O'Riordan KJ, Cowan CSM, Sandhu KV, Bastiaanssen TFS, Boehme M, Codagnone MG, Cussotto S, Fulling C, Golubeva AV, Guzzetta KE, Jaggar M, Long-Smith CM, Lyte JM, Martin JA, Molinero-Perez A, Moloney G, Morelli E, Morillas E, O'Connor R, Cruz-Pereira JS, Peterson VL, Rea K, Ritz NL, Sherwin E, Spichak S, Teichman EM, van de Wouw M, Ventura-Silva AP, Wallace-Fitzsimons SE, Hyland N, Clarke G, Dinan TG, 2019 The microbiota-gut-brain axis. Physiol. Rev 99, 1877–2013. [PubMed: 31460832]

Derrien M, Alvarez AS, de Vos WM, 2019 The gut microbiota in the first decade of life. Trends Microbiol 27, 997–1010. [PubMed: 31474424]

Desbonnet L, Clarke G, Shanahan F, Dinan TG, Cryan JF, 2014 Microbiota is essential for social development in the mouse. Mol. Psychiatry 19, 146–148. [PubMed: 23689536]

Donovan JD, Bauer L, Fahey GC Jr., Lee Y, 2017 In vitro digestion and fermentation of microencapsulated tributyrin for the delivery of butyrate. J. Food Sci 82, 1491–1499. [PubMed: 28485486]

Forbes JD, Van Domselaar G, Bernstein CN, 2016 Microbiome survey of the inflamed and noninflamed gut at different compartments within the gastrointestinal tract of inflammatory bowel disease patients. Inflamm. Bowel Dis 22, 817–825. [PubMed: 26937623]

Frohlich EE, Farzi A, Mayerhofer R, Reichmann F, Jacan A, Wagner B, Zinser E, Bordag N, Magnes C, Frohlich E, Kashofer K, Gorkiewicz G, Holzer P, 2016 Cognitive impairment by antibiotic-induced gut dysbiosis: Analysis of gut microbiota-brain communication. Brain, Behavior, and Immunity

Gacias M, Gaspari S, Santos PM, Tamburini S, Andrade M, Zhang F, Shen N, Tolstikov V, Kiebish MA, Dupree JL, Zachariou V, Clemente JC, Casaccia P, 2016 Microbiota-driven transcriptional changes in prefrontal cortex override genetic differences in social behavior. Elife 5.

Gareau MG, Wine E, Rodrigues DM, Cho JH, Whary MT, Philpott DJ, Macqueen G, Sherman PM, 2011 Bacterial infection causes stress-induced memory dysfunction in mice. Gut 60, 307–317. [PubMed: 20966022]

Ghaisas S, Maher J, Kanthasamy A, 2016 Gut microbiome in health and disease: Linking the microbiome-gut-brain axis and environmental factors in the pathogenesis of systemic and neurodegenerative diseases. Pharmacol. Ther 158, 52–62. [PubMed: 26627987]

Gomez-Hurtado I, Such J, Sanz Y, Frances R, 2014 Gut microbiota-related complications in cirrhosis. World J. Gastroenterol 20, 15624–15631. [PubMed: 25400446]

Good MA, Barnes P, Staal V, McGregor A, Honey RC, 2007 Context- but not familiarity-dependent forms of object recognition are impaired following excitotoxic hippocampal lesions in rats. Behav. Neurosci 121, 218–223. [PubMed: 17324066]

Goto Y, Yang CR, Otani S, 2010 Functional and dysfunctional synaptic plasticity in prefrontal cortex: roles in psychiatric disorders. Biol. Psychiatry 67, 199–207. [PubMed: 19833323]

Grayson MH, Camarda LE, Hussain SA, Zemple SJ, Hayward M, Lam V, Hunter DA, Santoro JL, Rohlfing M, Cheung DS, Salzman NH, 2018 Intestinal microbiota disruption reduces regulatory t cells and increases respiratory viral infection mortality through increased ifngamma production. Front. Immunol 9, 1587. [PubMed: 30042764]

Hill WD, Marioni RE, Maghzian O, Ritchie SJ, Hagenaars SP, McIntosh AM, Gale CR, Davies G, Deary IJ, 2019 A combined analysis of genetically correlated traits identifies 187 loci and a role for neurogenesis and myelination in intelligence. Mol. Psychiatry 24, 169–181. [PubMed: 29326435]

Hoban AE, Stilling RM, Ryan FJ, Shanahan F, Dinan TG, Claesson MJ, Clarke G, Cryan JF, 2016 Regulation of prefrontal cortex myelination by the microbiota. Transl. Psychiatry 6, e774. [PubMed: 27045844]

Hornig J, Frob F, Vogl MR, Hermans-Borgmeyer I, Tamm ER, Wegner M, 2013 The transcription factors Sox10 and Myrf define an essential regulatory network module in differentiating oligodendrocytes. PLoS Genet 9, e1003907. [PubMed: 24204311]

Huang Y, Shi X, Li Z, Shen Y, Shi X, Wang L, Li G, Yuan Y, Wang J, Zhang Y, Zhao L, Zhang M, Kang Y, Liang Y, 2018 Possible association of Firmicutes in the gut microbiota of patients with major depressive disorder. Neuropsychiatr. Dis. Treat 14, 3329–3337. [PubMed: 30584306]

Jangi S, Gandhi R, Cox LM, Li N, von Glehn F, Yan R, Patel B, Mazzola MA, Liu S, Glanz BL, Cook S, Tankou S, Stuart F, Melo K, Nejad P, Smith K, Topcuolu BD, Holden J, Kivisakk P, Chitnis T, De Jager PL, Quintana FJ, Gerber GK, Bry L, Weiner HL, 2016 Alterations of the human gut microbiome in multiple sclerosis. Nat. Commun 7, 12015. [PubMed: 27352007]

Kaakoush NO, 2015 Insights into the role of erysipelotrichaceae in the human host. Front. Cell. Infect. Microbiol 5, 84. [PubMed: 26636046]

Kaller MS, Lazari A, Blanco-Duque C, Sampaio-Baptista C, Johansen-Berg H, 2017 Myelin plasticity and behaviour-connecting the dots. Curr. Opin. Neurobiol 47, 86–92. [PubMed: 29054040]

Katoh K, Standley DM, 2013 MAFFT multiple sequence alignment software version 7: improvements in performance and usability. Mol. Biol. Evol 30, 772–780. [PubMed: 23329690]

Kho ZY, Lal SK, 2018 The human gut microbiome – a potential controller of wellness and disease. Front. Microbiol 9, 1835. [PubMed: 30154767]

Lebel C, Gee M, Camicioli R, Wieler M, Martin W, Beaulieu C, 2012 Diffusion tensor imaging of white matter tract evolution over the lifespan. Neuroimage 60, 340–352. [PubMed: 22178809]

Leclercq S, Mian FM, Stanisz AM, Bindels LB, Cambier E, Ben-Amram H, Koren O, Forsythe P, Bienenstock J, 2017 Low-dose penicillin in early life induces long-term changes in murine gut microbiota, brain cytokines and behavior. Nat. Commun 8, 15062. [PubMed: 28375200]

Liu H, Zhang JJ, Li X, Yang Y, Xie XF, Hu K, 2015 Post-occlusion administration of sodium butyrate attenuates cognitive impairment in a rat model of chronic cerebral hypoperfusion. Pharmacol. Biochem. Behav 135, 53–59. [PubMed: 26013850]

Lozupone C, Lladser ME, Knights D, Stombaugh J, Knight R, 2011 UniFrac: an effective distance metric for microbial community comparison. The ISME journal 5, 169–172. [PubMed: 20827291]

Lu QR, Sun T, Zhu Z, Ma N, Garcia M, Stiles CD, Rowitch DH, 2002 Common developmental requirement for Olig function indicates a motor neuron/oligodendrocyte connection. Cell 109, 75–86. [PubMed: 11955448]

Makki K, Deehan EC, Walter J, Backhed F, 2018 The impact of dietary fiber on gut microbiota in host health and disease. Cell Host Microbe 23, 705–715. [PubMed: 29902436]

Mandal S, Van Treuren W, White RA, Eggesbo M, Knight R, Peddada SD, 2015 Analysis of composition of microbiomes: a novel method for studying microbial composition. Microb. Ecol. Health Dis 26, 27663. [PubMed: 26028277]

Mitew S, Hay CM, Peckham H, Xiao J, Koenning M, Emery B, 2014 Mechanisms regulating the development of oligodendrocytes and central nervous system myelin. Neuroscience 276, 29–47. [PubMed: 24275321]

Morrison DJ, Preston T, 2016 Formation of short chain fatty acids by the gut microbiota and their impact on human metabolism. Gut Microbes 7, 189–200. [PubMed: 26963409]

Mumby DG, Gaskin S, Glenn MJ, Schramek TE, Lehmann H, 2002 Hippocampal damage and exploratory preferences in rats: memory for objects, places, and contexts. Learn. Mem 9, 49–57. [PubMed: 11992015]

Norman G, Eacott MJ, 2004 Impaired object recognition with increasing levels of feature ambiguity in rats with perirhinal cortex lesions. Behav. Brain Res 148, 79–91. [PubMed: 14684250]

Novotny M, Klimova B, Valis M, 2019 Microbiome and cognitive impairment: can any diets influence learning processes in a positive way? Front. Aging Neurosci 11, 170. [PubMed: 31316375]

Ntranos A, Casaccia P, 2018 The microbiome-gut-behavior axis: crosstalk between the gut microbiome and oligodendrocytes modulates behavioral responses. Neurotherapeutics 15, 31–35. [PubMed: 29282673]

O'Rourke M, Gasperini R, Young KM, 2014 Adult myelination: wrapping up neuronal plasticity. Neural Regen. Res 9, 1261–1264. [PubMed: 25221576]

Ormerod KL, Wood DL, Lachner N, Gellatly SL, Daly JN, Parsons JD, Dal'Molin CG, Palfreyman RW, Nielsen LK, Cooper MA, Morrison M, Hansbro PM, Hugenholtz P, 2016 Genomic characterization of the uncultured Bacteroidales family S24–7 inhabiting the guts of homeothermic animals. Microbiome 4, 36. [PubMed: 27388460]

Osaka T, Moriyama E, Arai S, Date Y, Yagi J, Kikuchi J, Tsuneda S, 2017 Meta-analysis of fecal microbiota and metabolites in experimental colitic mice during the inflammatory and healing phases. Nutrients 9.

Pittayanon R, Lau JT, Leontiadis GI, Tse F, Yuan Y, Surette M, Moayyedi P, 2020 Differences in gut microbiota in patients with vs without inflammatory bowel diseases: a systematic review. Gastroenterology 158 (930–946), e931.

Price MN, Dehal PS, Arkin AP, 2010 FastTree 2–approximately maximum-likelihood trees for large alignments. PLoS ONE 5, e9490. [PubMed: 20224823]

Pusceddu MM, Barboza M, Keogh CE, Schneider M, Stokes P, Sladek JA, Kim HJD, Torres-Fuentes C, Goldfild LR, Gillis SE, Brust-Mascher I, Rabasa G, Wong KA, Lebrilla C, Byndloss MX, Maisonneuve C, Baumler AJ, Philpott DJ, Ferrero RL, Barrett KE, Reardon C, Gareau MG, 2019a

Nod-like receptors are critical for gut-brain axis signalling in mice. J. Physiol 597, 5777–5797. [PubMed: 31652348]

Pusceddu MM, Stokes PJ, Wong A, Gareau MG, Genetos DC, 2019b Sexually dimorphic influence of neonatal antibiotics on bone. J. Orthop. Res 37, 2122–2129. [PubMed: 31228216]

Quast C, Pruesse E, Yilmaz P, Gerken J, Schweer T, Yarza P, Peplies J, Glockner FO, 2013 The SILVA ribosomal RNA gene database project: improved data processing and web-based tools. Nucleic Acids Res 41, D590–596. [PubMed: 23193283]

Rao M, Nelms BD, Dong L, Salinas-Rios V, Rutlin M, Gershon MD, Corfas G, 2015 Enteric glia express proteolipid protein 1 and are a transcriptionally unique population of glia in the mammalian nervous system. Glia 63, 2040–2057. [PubMed: 26119414]

Ren T, Gao Y, Qiu Y, Jiang S, Zhang Q, Zhang J, Wang L, Zhang Y, Wang L, Nie K, 2020 Gut microbiota altered in mild cognitive impairment compared with normal cognition in sporadic Parkinson's disease. Front. Neurol 11, 137. [PubMed: 32161568]

Round JL, Mazmanian SK, 2009 The gut microbiota shapes intestinal immune responses during health and disease. Nat. Rev. Immunol 9, 313–323. [PubMed: 19343057]

Sharma S, Taliyan R, Singh S, 2015 Beneficial effects of sodium butyrate in 6-OHDA induced neurotoxicity and behavioral abnormalities: modulation of histone deacetylase activity. Behav. Brain Res 291, 306–314. [PubMed: 26048426]

Sharon G, Sampson TR, Geschwind DH, Mazmanian SK, 2016 The central nervous system and the gut microbiome. Cell 167, 915–932. [PubMed: 27814521]

Smith BJ, Miller RA, Ericsson AC, Harrison DC, Strong R, Schmidt TM, 2019 Changes in the gut microbiome and fermentation products concurrent with enhanced longevity in acarbose-treated mice. BMC Microbiol 19, 130. [PubMed: 31195972]

Stilling RM, van de Wouw M, Clarke G, Stanton C, Dinan TG, Cryan JF, 2016 The neuropharmacology of butyrate: the bread and butter of the microbiota-gutbrain axis? Neurochem. Int 99, 110–132. [PubMed: 27346602]

van de Wouw M, Boehme M, Lyte JM, Wiley N, Strain C, O'Sullivan O, Clarke G, Stanton C, Dinan TG, Cryan JF, 2018 Short-chain fatty acids: microbial metabolites that alleviate stress-induced brain-gut axis alterations. J. Physiol 596, 4923–4944. [PubMed: 30066368]

Vieira EL, Leonel AJ, Sad AP, Beltrao NR, Costa TF, Ferreira TM, Gomes-Santos AC, Faria AM, Peluzio MC, Cara DC, Alvarez-Leite JI, 2012 Oral administration of sodium butyrate attenuates inflammation and mucosal lesion in experimental acute ulcerative colitis. J. Nutr. Biochem 23, 430–436. [PubMed: 21658926]

Warburton EC, Brown MW, 2015 Neural circuitry for rat recognition memory. Behav. Brain Res. 285, 131–139. [PubMed: 25315129]

Williamson JM, Lyons DA, 2018 Myelin dynamics throughout life: an ever-changing landscape? Front. Cell. Neurosci 12, 424. [PubMed: 30510502]

Yan J, Charles JF, 2018 Gut microbiota and IGF-1. Calcif. Tissue Int 102, 406–414. [PubMed: 29362822]

Yoo BB, Mazmanian SK, 2017 The enteric network: interactions between the immune and nervous systems of the gut. Immunity 46, 910–926. [PubMed: 28636959]

Zhao X, Zhang Z, Hu B, Huang W, Yuan C, Zou L, 2018 Response of gut microbiota to metabolite changes induced by endurance exercise. Front. Microbiol 9, 765. [PubMed: 29731746]

Zhuang M, Shang W, Ma Q, Strappe P, Zhou Z, 2019 Abundance of probiotics and butyrate-production microbiome manages constipation via short-chain fatty acids production and hormones secretion. Mol. Nutr. Food Res 63, e1801187. [PubMed: 31556210]

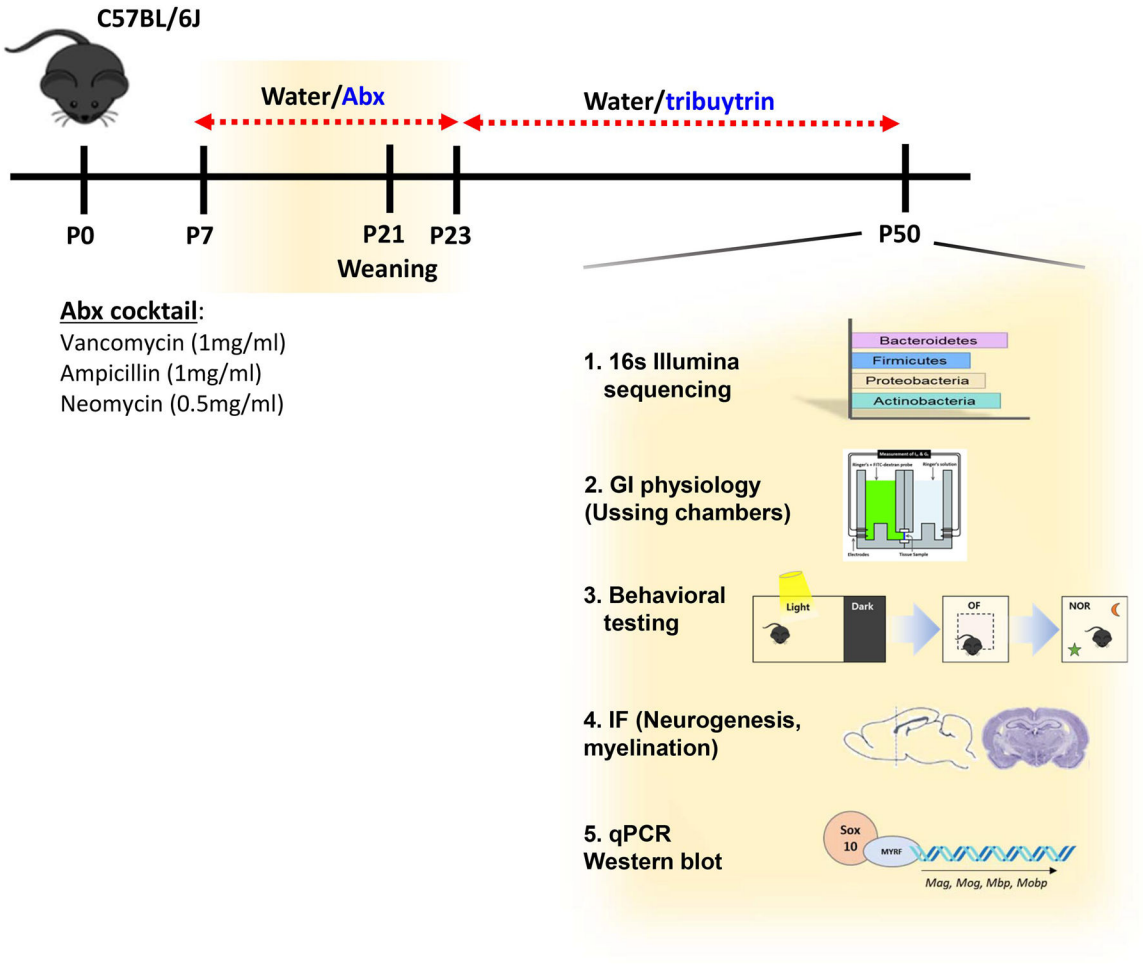

Fig. 1.

Study Design. C57BL/6J mice were orally gavaged with antibiotic (Abx) cocktail or water (vehicle) from postnatal (P) day 7 to P23. From P24 to P50, mice were given normal water or tributyrin. Upon euthanasia, fecal pellets were used to analyze gut bacterial community analysis via 16s Illumina sequencing. Tissue samples such as prefrontal cortex (PFC), hippocampus, and ileum were used for qPCR or western blot. Immunofluorescence was performed in the medial-PFC. Ileal physiology was analyzed via Ussing chambers. Behavioral tests were performed to assess cognition and anxiety-like behavior. Neurogenesis was analyzed via immunofluorescence of dorsal hippocampus.

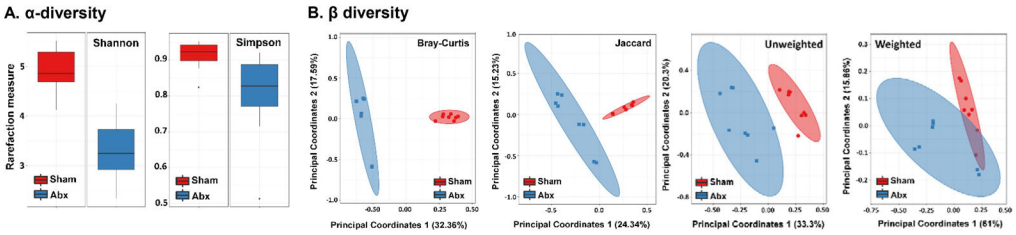

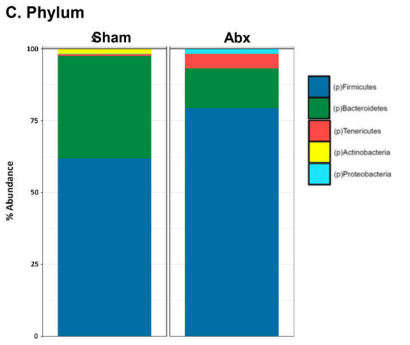

Taxa	Sham	Abx	P value
Actinobacteria	1.66 ± 0.65	0.01 ± 0.01	***
Bacteroidetes	35.06 ± 3.75	13.86 ± 9.04	***
Firmicutes	60.55 ± 3.24	79.46 ± 8.6	***
Proteobacteria	0.15 ± 0.03	1.65 ± 0.98	***
Tenericutes	0.67 ± 0.21	5 ± 3.27	***
Total	98.086	99.983	

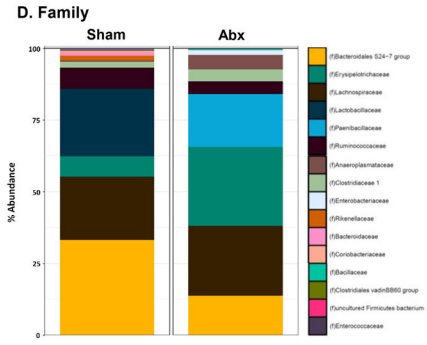

Taxa	Sham	Abx	P value
Alcaligenaceae	0.15 ± 0.03	0 ± 0	***
Anaeroplasmataceae	0.45 ± 0.23	4.99 ± 3.27	***
Bacillaceae	0.01 ± 0.01	0.37 ± 0.14	***
Bacteroidaceae	1.07 ± 0.27	0 ± 0	**
Bacteroidales S24-7 group	32.12 ± 3.73	13.79 ± 9.06	***
Clostridiaceae 1	2.08 ± 1.37	4.12 ± 2.38	***
Clostridiales vadinBB60 group	0.32 ± 0.06	0.04 ± 0.03	***
Coriobacteriaceae	0.56 ± 0.21	0 ± 0	***
Enterobacteriaceae	0.01 ± 0.01	1.64 ± 0.98	***
Enterococcaceae	0 ± 0	0.18 ± 0.09	***
Erysipelotrichaceae	6.75 ± 0.87	27.48 ± 9.61	***
Family XIII	0.09 ± 0.02	0 ± 0	***
Lachnospiraceae	21.26 ± 1.71	24.31 ± 3.24	**
Lactobacillaceae	22.19 ± 3.79	0.01 ± 0.01	***
Paenibacillaceae	0 ± 0	18.48 ± 7.46	***
Rikenellaceae	1.52 ± 0.3	0 ± 0	**
Ruminococcaceae	7.14 ± 1.34	4.42 ± 2.23	***
Uncultured Firmicutes bac.	0.19 ± 0.09	0 ± 0	***
.098	0.05 ± 0.02 ±	0 ± 0	
Total	96.258	99.841	

Fig. 2.

Neonatal Abx administration causes persistent gut dysbiosis in adulthood. (A) Shannon and Simpson indexes for α-diversity, (B) Bray-Curtis, Jaccard, and UniFrac (weighted and unweighted) indexes for β-diversity, (C) Phylum abundance and (D) Family abundance. Holm-Sidak; $^{**}p < 0.01$, ***p < 0.001; N = 12.

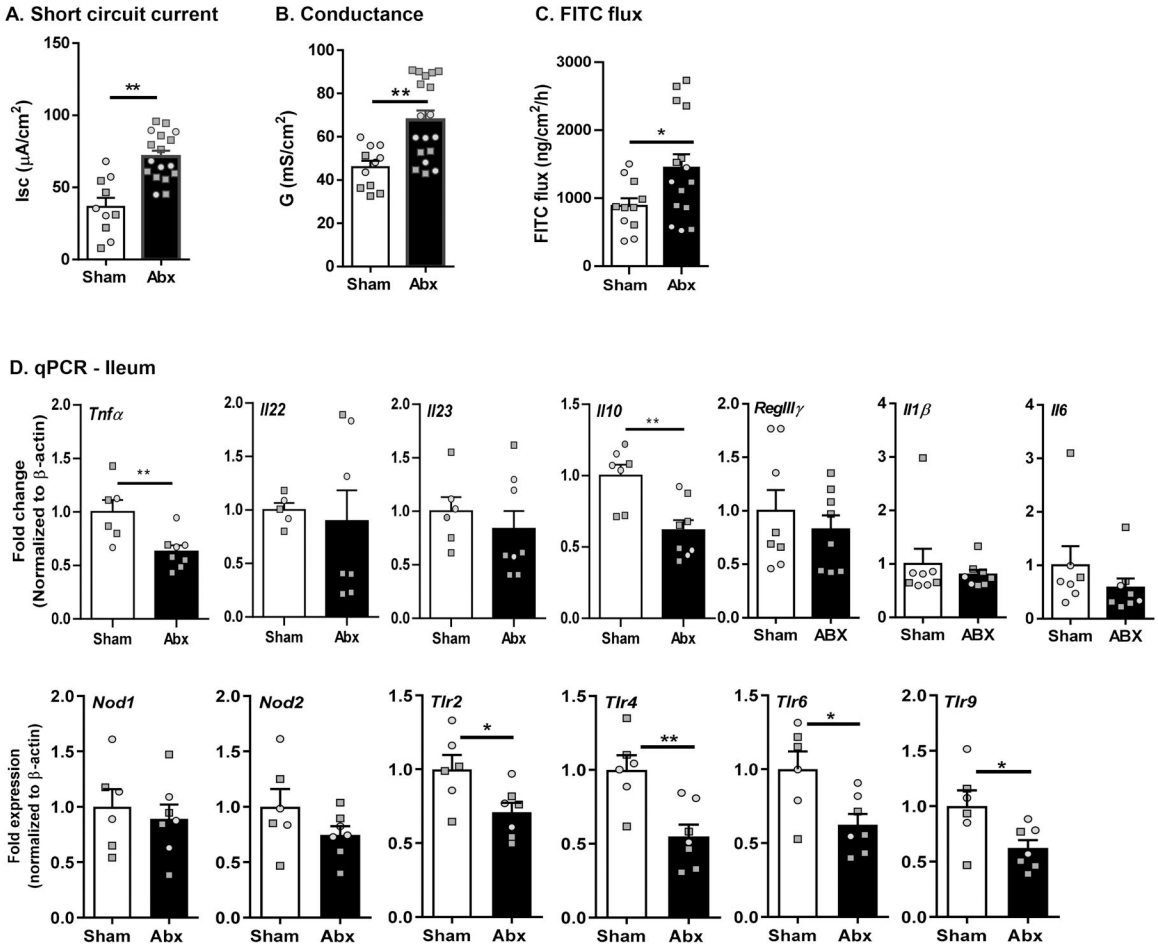

Fig. 3.

Neonatal Abx administration causes ileal pathophysiology without causing intestinal inflammation in adulthood. Ussing chamber studies assessed (A) short circuit current [Isc], (B) conductance (G) and (C) FITC flux in the ileum (N = 11–16). (D) Expression of immune-related genes (cytokines, pattern recognition receptors) in the ileum by qPCR (N = 8). Females denoted as light grey circles, and males as dark grey squares. Students T-test, *$p < 0.05$, **$p < 0.01$.

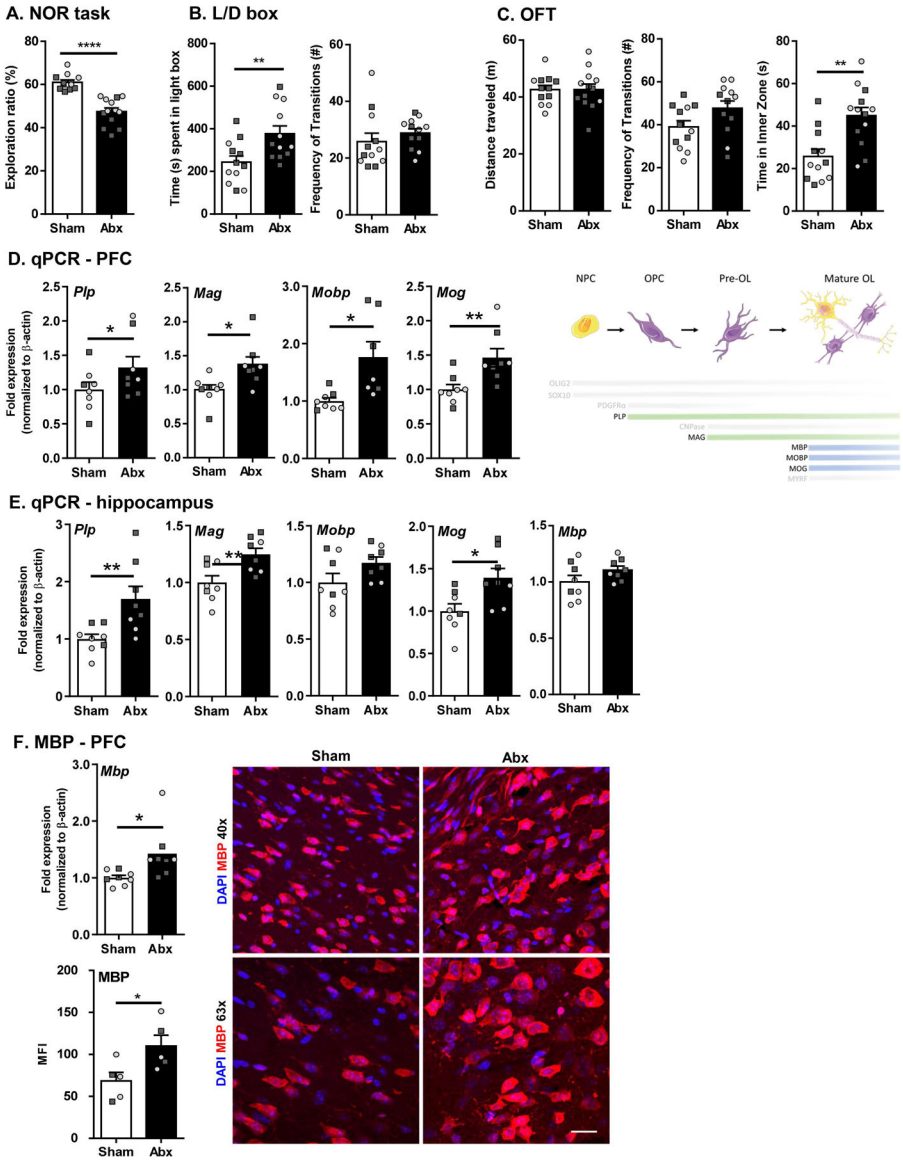

Fig. 4.

Neonatal Abx administration leads to behavioral deficits and myelin dysregulation in adulthood. (A) Novel object recognition task. (B) Light/dark box; *(i)* % time spent in the light, *(ii)* Frequency of transitions. (C) Open field test; *(i)* Distance travelled, *(ii)* Frequency of transitions, *(iii)* Time in inner zone. Expression of myelin-associated genes in the prefrontal cortex (PFC; D) and hippocampus (E). N = 14–16 for behavioral tests; N = 7–8 for qPCR; N = 5 for IF. (F) Gene expression (N = 8) and IF (N = 5) for MBP in the PFC region. DAPI in blue and MBP in red. Scale bar 20 μm. Unpaired T-test *p < 0.05. Females denoted as light grey circles, and males as dark grey squares. Students T-test, $*p < 0.05$, $**p < 0.01$.

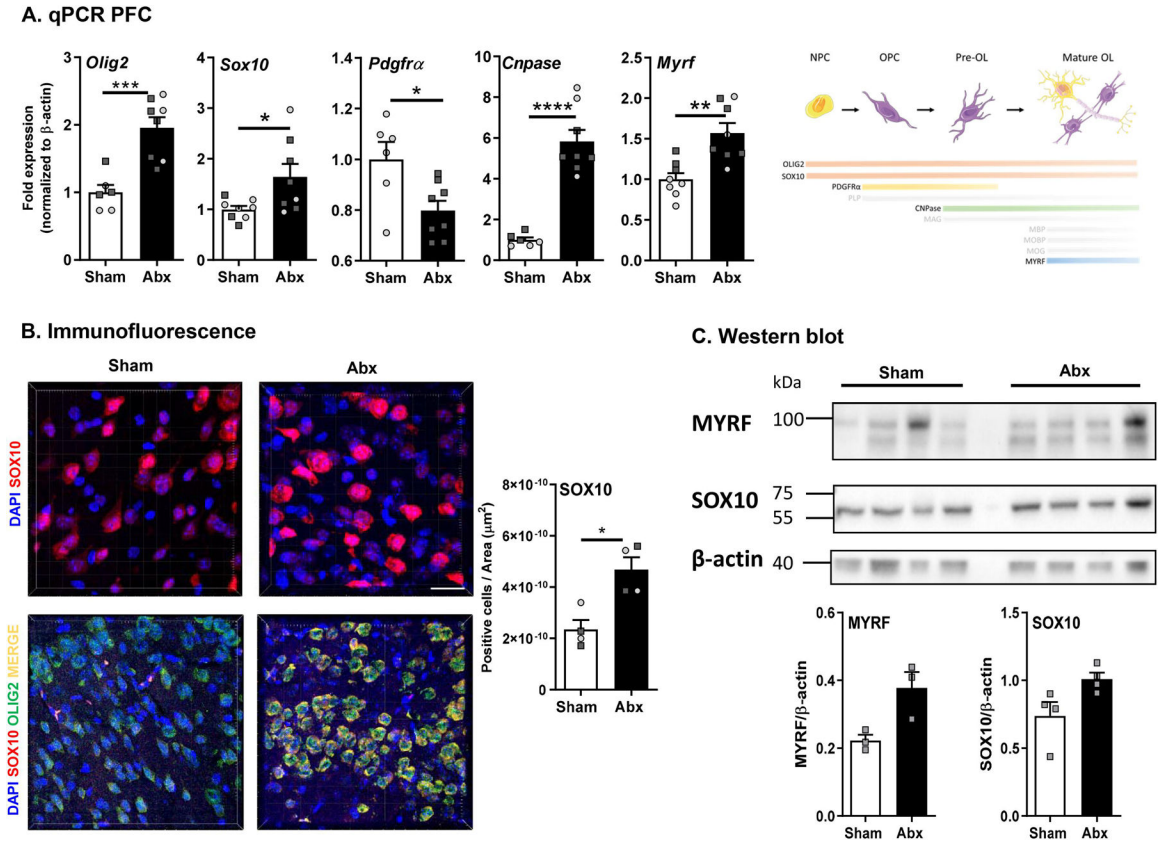

Fig. 5.

Neonatal Abx administration leads to maturation and differentiation of oligodendrocytes. (A) mRNA expression of oligodendrocyte lineage-specific markers in the pre-frontal cortex (PFC) (N = 7–8). (B) Immunofluorescence for SOX10 (63x) expression in the PFC (N = 4). DAPI in blue and SOX10 in red. Scale bar 20 μm. Unpaired T-test $*p < 0.05$; co-localisation staining of OLIG2 and SOX10 (40x) in the PFC region (N = 4). DAPI in blue, SOX10 in red, OLIG2 in green, merge in yellow). Scale bar 50 μm. (C) Western blot and densitometric analysis for MYRF, SOX10 and β-actin (N = 5). Females denoted as light grey circles, and males as dark grey squares. Student's T-test $*p \leq 0.05$.

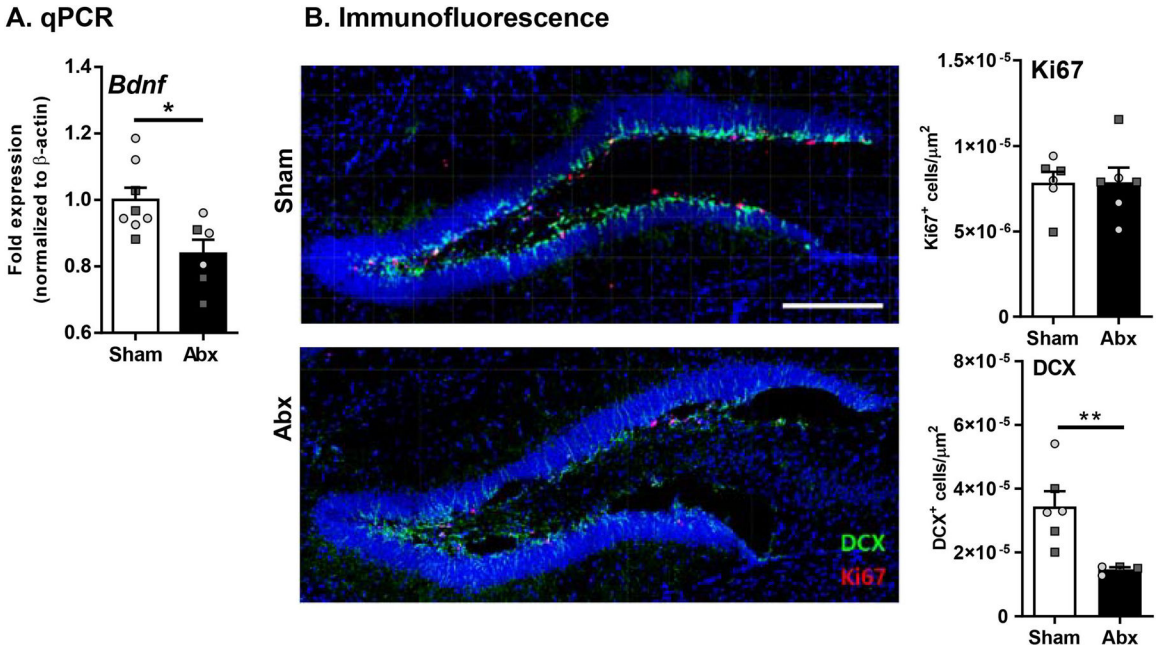

Fig. 6.

Neonatal Abx administration causes dysregulation of IGF signaling and neurogenesis. (A) BDNF gene expression in the pre-frontal cortex (PFC) (N = 6–8) (B) Expression of DCX (green) and Ki67 (red) in the hippocampus (20x) (N = 6). Females denoted as light grey circles, and males as dark grey squares. Students T-test, $*p \leq 0.05$, $**p < 0.01$.

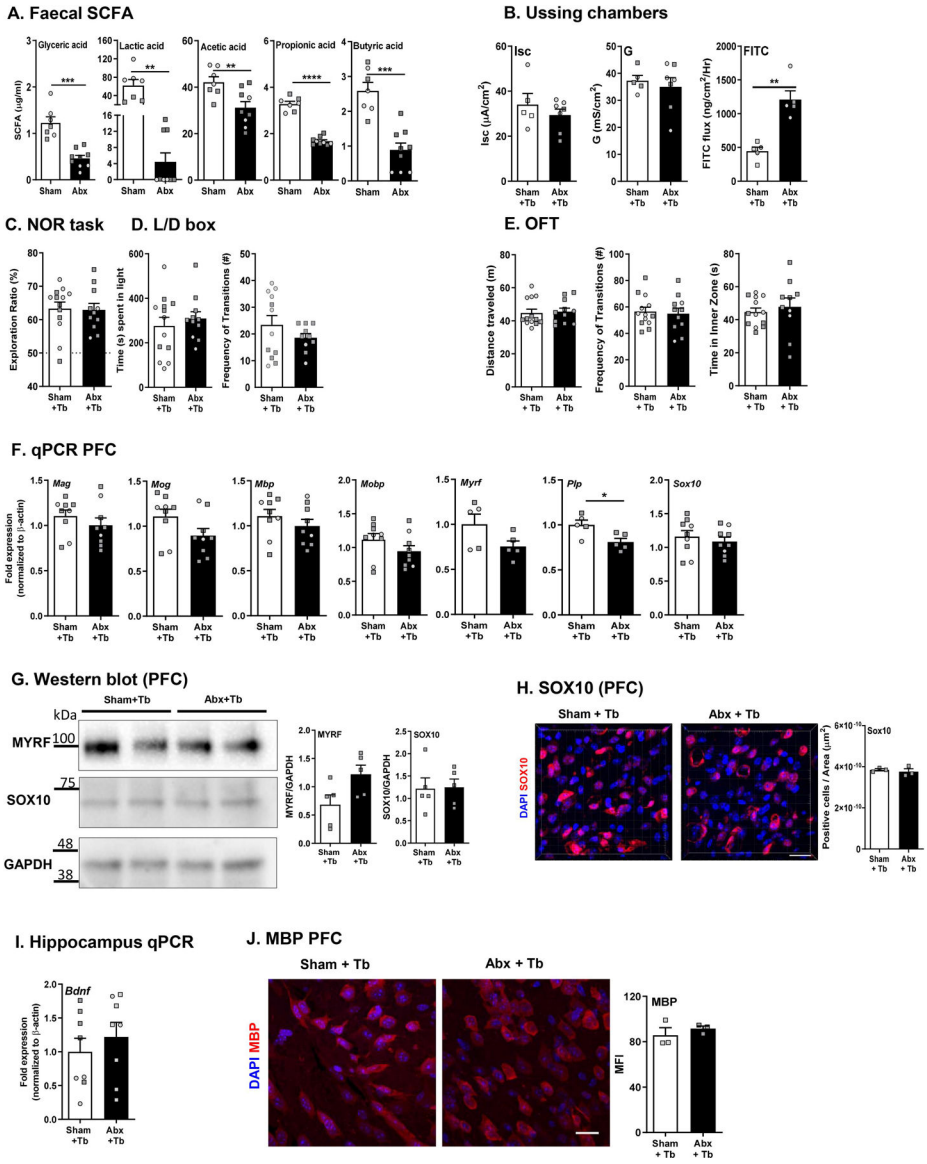

Fig. 7.

Tributyrin supplementation rescues behavior, intestinal physiology, and myelin dysregulation in adulthood. (A) Short chain fatty acid concentrations in fecal pellets as measured by mass spectrometry. (B) Ussing chamber studies for short-circuit current (Isc), conductance (G) and flux of FITC dextran. (C) Novel object recognition (NOR) task. (D) Light/dark box; *(i)* % time spent in the light, *(ii)* Frequency of transitions. (E) Open field task (OFT); *(i)* Distance travelled, *(ii)* Frequency of transitions, *(iii)* Time in inner zone. N = 11–14 (F) Expression of myelin-related genes in the pre-frontal cortex (PFC) (N = 8–9). (G) Western blot and densitometric analysis for MYRF, SOX10 and GAPDH in the PFC (N = 5). (H) Immunofluorescence of SOX10 (63x) in the PFC region (N = 4). DAPI in blue and SOX10 in red. Scale bar 20 μm. (I) Hippocampal *Bdnf* mRNA expression (N = 8–9). (J) Immunofluorescence of MBP (63x) in the PFC region (N = 3) DAPI in blue and MBP in

red. Scale bar 20 μm. Females denoted as light grey circles, and males as dark grey squares. Student's T-test. *$p < 0.05$.

Table 1

Primer sequences used in qPCR.

	Forward	Reverse
Mag	TGAGACGGAGAGGGAGTTTG	CTCGTCTGGGTGATGTAGCA
Mog	CTGTTTGTTATTGTGCCTGTTCTTG	AGTCTTCGGTGCAGCCAGTT
Mbp	ACACACGAGAACTACCCATTATGG	AGAAATGGACTACTGGGTTTTCATCT
Mobp	AACTCCAAGCGTGAGATCGT	CTCGGTCACTTCTTCCTTGG
Plp	CCCACCCCTATCCGCTAGTT	CAGGAAAAAAAGCACCATTGTG
Myrf	GCATGGGCACCGCCCCTAAG	GGGGCGAGTCTGGCAGTGTG
Sox10	TGGACCGCACACCTTGGGACA	ACGCCCACCTCCTCCGACCT
Igf1	GGACCGAGGGGCTTTTACTTC	AGTCTTGGGCATGTCAGTGTGG
Igf2	CGCTTCAGTTTGTCTGTTCG	GGAAGTACGGCCTGAGAGGTA
Igf1r	AGGAGAAGCCCATGTGTGAG	GTGTTGTCGTCCGGTGTGT
Igf2r	GGGAAGCTGTTGACTCCAAAA	GCAGCCCATAGTGGTGTTGAA
Igfbp1	CCATTGCCACTACTATCTACTCA	GCAGCCTTTGCCTCTTC
Igfbp3	AATGGCCGCGGGTTCTGC	TTCTGG GTGTCTGTGCTTTGAG
Bdnf	TGCAGGGGCATAGACAAAAGG	CTTATGAATCGCCAGCCAATTCTC
Sert	CGCCTCCCGCAGAGC	AAGGTGTGGTCTCCATGCTG
Tph2	TCGAAATCTTCGTGGACTGC	CGGATTCAGGGTCACAATG
IFNγ	TGCTGATGGCCTGATTGTCT	GCCACGGCACAGTCATTGA
iκbα	GAAGCCGCTGACCATGGAA	GATCACAGCCAAGTGGAGTGGA
Il23	TTCAGATGGGCATGAATGTTTCT	CCAAATCCGAGCTGTTGTTCTAT
il10	GCTCTTACTGACTGGCATGAG	CGCAGCTCTAGGAGCATGTG
il1β	CTGTGACTCATGGGATGATGATG	CGGAGCCTGTAGTGCAGTTG
il6	TAGTCCTTCCTACCCCAATTTCC	TTGGTCCTTAGCCACTCCTTC
regiiiγ	TTCCTGTCCTCCATGATCAAAA	CATCCACCTCTGTTGGGTTCA
tnfa	CCCTCACACTCAGATCATCTTCT	GCTACGACGTGGGCTACAG
BActin	GGCTGTATTCCCCTCCATCG	CCAGTTGGTAACAATGCCATGT

Table 2

SCFA levels.

	Sham	Abx	Sham + Tb	Abx + Tb
Cecum (μMol/g)				
Glyceric acid	47.42 ± 2.961	19.17 ± 5.328 *	24.71 ± 3.748 *	18.86 ± 2.044 *
Lactic acid	3.534 ± 0.5094	0.4402 ± 0.2024 *	4.767 ± 0.8979	1.235 ± 0.5047 *#
Acetic acid	16.34 ± 0.8928	9.919 ± 2.662 *	23.8 ± 3.853	4.747 ± 1.029 *#
Propionic acid	1.859 ± 0.1723	0.4407 ± 0.07178 *	3.476 ± 0.4848	1.018 ± 0.2975 *#
Butyric acid	14.28 ± 1.973	6.691 ± 1.365 *	8.543 ± 1.485	3.403 ± 0.5179
Fecal (μMol/g)				
Glyceric acid	1.228 ± 0.1274	0.4602 ± 0.06495 *	0.606 ± 0.103 *	0.4265 ± 0.07653 *
Lactic acid	52.52 ± 9.956	4.427 ± 2.213 *	40.12 ± 9.062	5.887 ± 3.768 *#
Acetic acid	42.13 ± 2.356	31.19 ± 2.6 *	55.54 ± 7.05	41.48 ± 3.752
Propionic acid	3.279 ± 0.1129	1.679 ± 0.05846 *	2.516 ± 0.6894	1.59 ± 0.06127 *
Butyric acid	2.698 ± 0.2735	0.8903 ± 0.1984 *	0.8988 ± 0.1802 *	0.2775 ± 0.01434 *

* $p < 0.05$ vs sham

# $p < 0.05$ vs Sham + Tb

N = 5–7.